

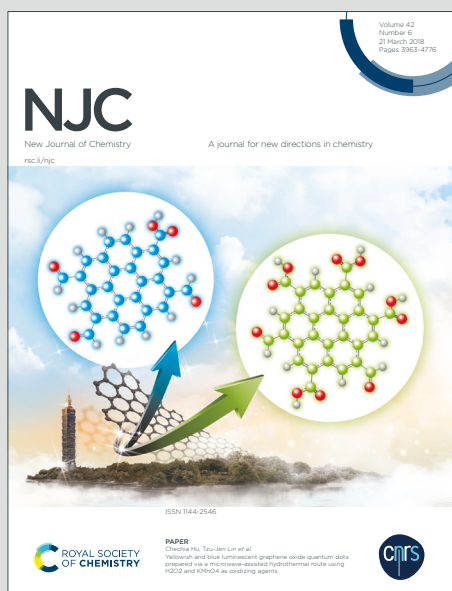
# NJC

New Journal of Chemistry

Accepted Manuscript

A journal for new directions in chemistry

This article can be cited before page numbers have been issued, to do this please use: K. Jelínková, J. Kovaevi, E. Wrzecionková, Z. Prucková, M. Rouchal, L. Dastychová and R. Vícha, *New J. Chem.*, 2020, DOI: 10.1039/D0NJ00738B.



This is an Accepted Manuscript, which has been through the Royal Society of Chemistry peer review process and has been accepted for publication.

Accepted Manuscripts are published online shortly after acceptance, before technical editing, formatting and proof reading. Using this free service, authors can make their results available to the community, in citable form, before we publish the edited article. We will replace this Accepted Manuscript with the edited and formatted Advance Article as soon as it is available.

You can find more information about Accepted Manuscripts in the [Information for Authors](#).

Please note that technical editing may introduce minor changes to the text and/or graphics, which may alter content. The journal's standard [Terms & Conditions](#) and the [Ethical guidelines](#) still apply. In no event shall the Royal Society of Chemistry be held responsible for any errors or omissions in this Accepted Manuscript or any consequences arising from the use of any information it contains.

# Binding study on 1-adamantylalkyl(benz)imidazolium salts towards cyclodextrins and cucurbit[*n*]urils

View Article Online  
DOI: 10.1039/D0NJ00738B

Kristýna Jelínková, Jelica Kovačević, Eva Wrzcionková, Zdeňka Prucková, Michal Rouchal, Lenka Dastychová, and Robert Vícha\*

Department of Chemistry, Faculty of Technology, Tomas Bata University in Zlín, Vavrečkova 275, 760 01 Zlín, Czech Republic

\*Corresponding author. Tel.: +420-576031103; e-mail: rvicha@utb.cz

## Abstract

Multitopic guests are used as key components of molecular triggers, switchers, sensors, or reactors in recent supramolecular chemistry studies. The increasing complexity of these compounds correlates with the need for versatile, synthetically available binding motifs (building blocks) with tuneable supramolecular properties. The utilisation of a favoured 1-adamantylmethyl moiety within ammonium, imidazolium and pyridinium salts is sometimes restricted by synthetic difficulties most likely related to adamantane cage bulkiness. Therefore, we prepared a series of new adamantylated (benz)imidazolium salts with longer flexible linkers between the adamantane cage and cationic moiety. We tested supramolecular properties of these binding motifs towards natural cyclodextrins  $\alpha$ -CD,  $\beta$ -CD and  $\gamma$ -CD and cucurbit[*n*]urils ( $n=7,8$ ) using NMR, mass spectrometry and titration calorimetry. All tested guests formed 1:1 complexes with abovementioned hosts retaining binding strengths, selectivity, and complex geometries in comparison to the parent methylene-linked homologues. We did not confirm our original concern that longer linkers would negatively affect the binding strength towards CBns due to reducing the ion-dipole interaction contribution. Therefore, we believe that adamantylalkyl imidazolium binding motifs can be used for multitopic supramolecular guest construction.

**Keywords:** adamantane, cucurbit[*n*]uril, cyclodextrins, host-guest systems, supramolecular chemistry.

## 1. Introduction

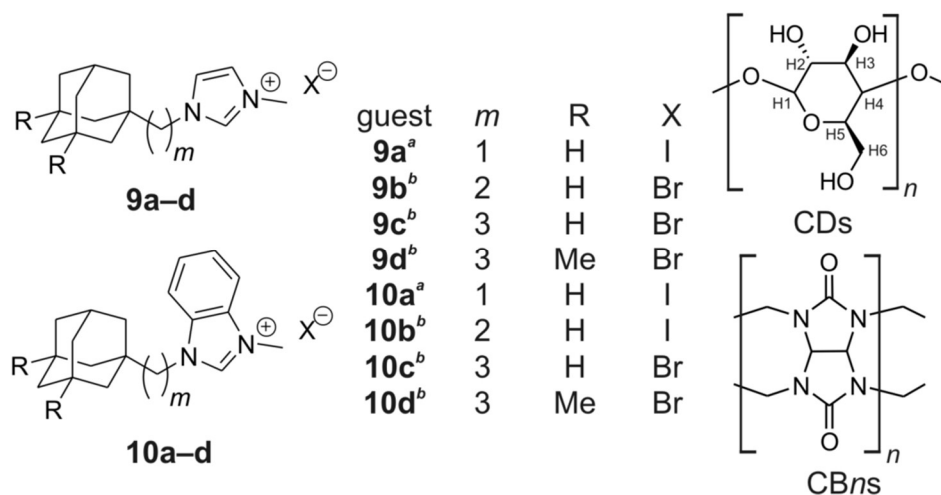
Host-guest chemistry plays a significant role in the world of supramolecular chemistry. Well-defined and structurally organised supramolecular systems are formed employing non-covalent interactions in the sense of molecular recognition and self-assembly concept. In specific situations, when axle-like guests consist of more than one binding site (generally, *n* sites) with suitable affinities towards particular macrocycles, stable supramolecular arrangements can be prepared in a [*n*]pseudorotaxane manner.<sup>1</sup> Indeed, the binding strengths of particular sites must be well-tuned. Therefore, characterisation of binding properties of model guests is fundamental for designing more complex multitopic guests which can have advanced functions. A properly organised tritopic guest serves as an axis of an enantioselective reactor made of [4]rotaxane with a chiral cavity of  $\gamma$ -CD, which contributes (*Z,E*)-1,3-cyclooctadiene up to 15.3% ee via photoisomerisation of (*Z,Z*)-1,3-cyclooctadiene with the highest value for enantioselectivity of

the supramolecular isomerisation.<sup>2</sup> Another advanced supramolecular system is a doubly photoresponsive multitopic guest composed of azobenzene and stilbene moieties that can be isomerised separately with UV light of different wavelength.<sup>3</sup> The molecular shuttle of  $\alpha$ -CD is driven by photochemical reversible isomerisation of photosensitive units.

Natural and inexpensive cyclodextrins (CDs) and highly symmetric and selective cucurbit[*n*]urils (CBns) are the most extensively studied families of macrocyclic hosts. Cyclodextrins are cyclic oligosaccharides which can be prepared by enzymatic decomposition of starch.<sup>4</sup> Molecules of the most common natural cyclodextrins,  $\alpha$ -,  $\beta$ - and  $\gamma$ -CD, consist of 6, 7 and 8 D-glucopyranoside units linked by  $\alpha(1\rightarrow4)$  glycosidic bonds, respectively. These macrocycles adopt a hollow truncated cone with non-symmetric portals shape. Cyclodextrins have attracted the attention for their biocompatibility, nontoxicity and capability of forming inclusion complexes with positively charged or neutral guests. Since cyclodextrins are inherently chiral, they have been employed in catalysis<sup>5</sup> or separation techniques.<sup>6</sup>

Cucurbit[*n*]urils are synthetic macrocycles oligomers prepared by condensation of *n* glycoluril units and formaldehyde.<sup>7</sup> Although the structure of CB6 was determined in 1980s,<sup>8</sup> the family of known CBns was enriched with CB5, CB7 and CB8, which were discovered by Kim in 2000.<sup>9</sup> CB*n* molecules are highly rigid, barrel-like shaped convex cylinders with two symmetric carbonyl-rimmed portals and hydrophobic cavity. The geometry and electronic properties of CBns are best suited for positively charged guests derived from a hydrocarbon parent skeleton. Geometric compatibility of the host interior cavity and nonpolar guest parent hydrocarbon combined with positively charged moieties properly located in the centres of host portals can lead to highly stable host-guest complexes.<sup>10,11</sup> Particularly, CB7 forms ultrahigh-affinity host-guest pairs with dicationic derivatives of ferrocene<sup>12</sup> and cage hydrocarbons, such as adamantane,<sup>13,14</sup> diamantane,<sup>15,16</sup> bicyclo[2.2.2]octane<sup>13</sup> or cubane.<sup>17</sup>

Our research group focused on the synthesis and study of binding properties of various multitopic guests. We have reported several guests with terminal adamantane-based binding sites which were prepared via quaternisation using 1-adamantylmethyl iodide.<sup>18,19,20</sup> However, we faced serious synthetic difficulties, most likely related to the bulkiness of the adamantane cage, which disabled the preparation of some promising guests. Therefore, we decided to synthesise a series of model guests with an extended linker between the adamantane cage and cationic moiety. We prepared three methylimidazolium and three methylbenzimidazolium salts with 2-(1-adamantyl)ethyl, 3-(1-adamantyl)propyl and 3-(3,5-dimethyladamantan-1-yl)propyl substituents, respectively (see Figure 1 for structures). Subsequently, we concentrated on binding properties of the model guests towards CDs and CBns to examine whether ethylene and propylene linkers influence affinity towards macrocycles. The binding behaviour was investigated by means of NMR and mass spectrometry. Association constants were determined by isothermal titration calorimetry.

View Article Online  
DOI: 10.1039/D0NJ00738B

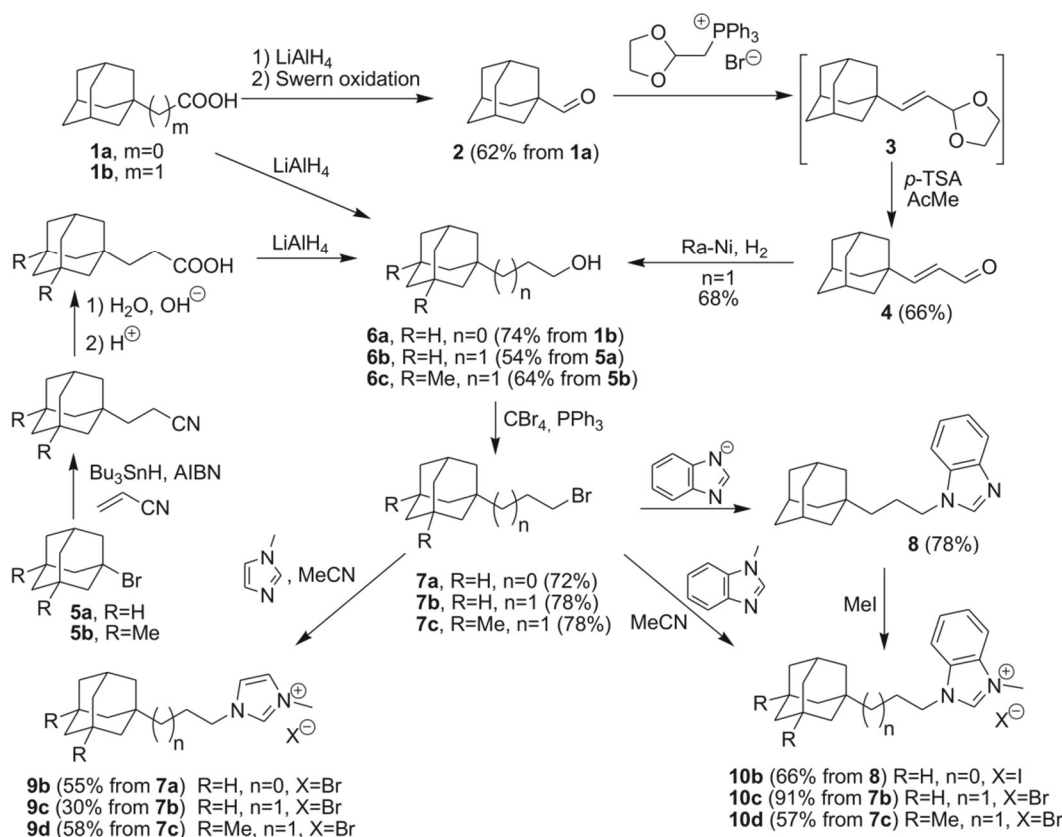
**Figure 1** Structures of the hosts ( $n=6,7,8$ ) and the guests under consideration (<sup>a</sup> published previously; <sup>b</sup> this study).

## 2. Results and Discussion

### 2.1 Chemistry

The adamantyl based imidazolium and benzimidazolium salts **9a** and **10a** with methylene linker between the adamantane cage and (benz)imidazolium cation (see Figure 1 for structures) were prepared in our previous work.<sup>21</sup> The (benz)imidazolium salts **9b–9d** and **10b–10d** were prepared according to synthetic pathways shown in Scheme 1. We synthesised the compound **6b** using two different pathways. The first pathway involved the radical addition of 1-bromoadamantane to the acrylonitrile, nitrile hydrolysis and reduction to produce alcohol **6b** in a moderate overall yield of 54%.<sup>22,23</sup> The alternative pathway started from adamantane-1-carboxylic acid (**1a**), which was transformed to the aldehyde **2** via subsequent reduction with  $\text{LiAlH}_4$  and Swern oxidation. Aldehyde **2** was reacted with oxolan-2-ylmethyl(triphenyl)phosphonium bromide under Wittig conditions to produce acetal **3**. Subsequent hydrolyses and hydrogenation afforded the critical intermediate 3-(1-adamantyl)propan-1-ol in the acceptable yield of 28% regarding the carboxylic acid **1a**. While the former approach was more efficient, the latter avoids handling of unpleasant organotin compounds. Alcohols **6a** and **6c** were obtained via a reduction from carboxylic acid **1b** and via the abovementioned three-step approach from 1-bromo-3,5-dimethyladamantane (**5b**), respectively. The alcohols **6** were converted to the corresponding bromoderivatives **7** via convenient Appel's bromination to avoid undesired elimination reactions. The ethylene (benz)imidazolium salts **9** and **10** are available from bromoderivatives **7** either by a sequence of *N*-substitution on the (benz)imidazole precursor and final methylation (as demonstrated for

**10b**) or directly by quaternisation using 1-methyl(benz)imidazole. Although both these methods provided comparable overall yields, the latter is of higher importance since it mimics the final introduction of terminal binding sites into molecules of multitopic ligands. Therefore, we demonstrated that bromides **7** could be used as quaternisation agents to provide final guests **9** and **10** in satisfactory yields.



**Scheme 1** The synthetic pathways leading to the guests under consideration.

## 2.2 Host-guest Studies

### 2.2.1 NMR experiments

We started our investigation of supramolecular properties through NMR experiments. Initially, we studied the behaviour of our (benz)imidazolium salts with host molecules  $\alpha$ -CD,  $\beta$ -CD,  $\gamma$ -CD, CB6, CB7 and CB8 using  $^1\text{H}$  NMR titration. It is a well-known phenomenon that CDs markedly deshield protons located inside their cavities. Since the most downfield shifted signals in all cases were that of adamantyl groups, we infer that guests **9b–9d** and **10b–10d** interact with cyclodextrins with their adamantane cages in inclusion manner.

**Table 1** Maximal complexation-induced shifts (CIS) for the most affected H-atoms of the guests.

guest	host	CIS <sub>max</sub> H( ) [ppm]	CIS <sub>max</sub> [ppm]
<b>9b</b> R=H	α-CD	0.107	
	β-CD	0.218	
	γ-CD	0.052	0.081 H( )
<b>9c</b> R=H	α-CD	0.108	
	β-CD	0.217	
	γ-CD	0.027	0.105 H( )
<b>9d</b> R=Me	α-CD	0.125	
	β-CD	0.226	
	γ-CD	0.089	
<b>10b</b> R=H	α-CD	0.127	
	β-CD	0.228	
	γ-CD	0.055	0.118 H( )
<b>10c</b> R=H	α-CD	0.120	
	β-CD	0.232	
	γ-CD	0.011	0.067 H( )
<b>10d</b> R=Me	α-CD	0.108 <sup>a</sup>	0.065 H( )
	β-CD	0.288 <sup>a</sup>	0.102 H( )
	γ-CD	0.097 <sup>a</sup>	0.127 H( )

<sup>a</sup> values were roughly estimated due to overlapping of the signals

Table 1 summarises the observed complexation induced shifts (CISs) for important guest H-atoms. As usual for inclusion complexes of adamantane-derived guests and CDs, the most affected H-atoms were those at bridgehead positions or the methyl substituents in positions 3 and 5 (numbering of the adamantyl substituent). However, it is worthy of attention that the H-atoms at the linker between the adamantane cage and (benz)imidazolium core were most influenced by complexation in the case of guests **9b**, **9c**, **10b** and **10c**. This fact indicates the different orientation of the binding partners. Surprisingly, maximum CIS observed for the interactions of all examined guests with α-CD were comparable with that for complexes with γ-CD. This trend positively correlates with the stability of the corresponding complexes, as can be seen in Table 1. Additionally, two-dimensional ROESY experiments show the interactions between adamantane hydrogens and hydrogens of the inner cavity of CDs for all examined cyclodextrins as depicted for the guest **10c** in Figure 2. The 1:1 stoichiometry of host-guest complexes with CDs was determined by Job plot in all cases as can be seen in Figures S79–S94.

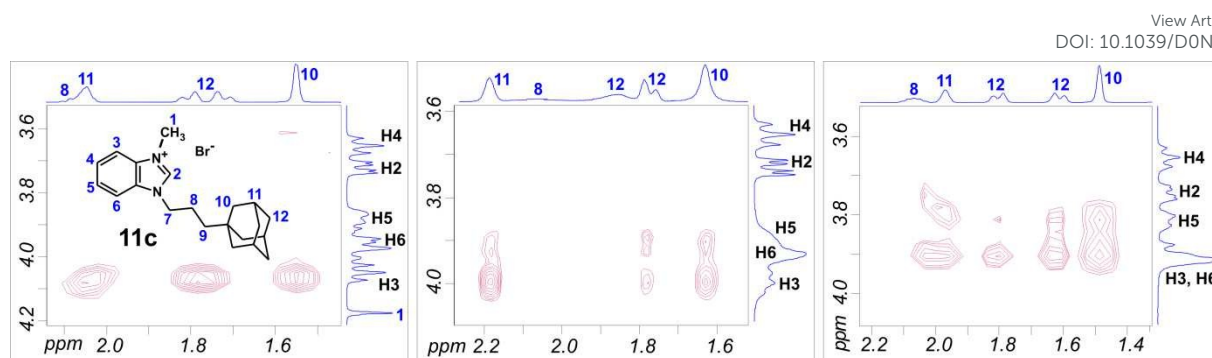


**Figure 2** Portions of ROESY spectra recorded for 1:1 mixtures of the guest **10c** and  $\alpha$ -CD,  $\beta$ -CD,  $\gamma$ -CD, respectively from left to right. Figure 1 illustrates the assignment of the CD's signals.

NMR titrations of guests **9b**, **9c**, **10b**, **10c** with CB7 revealed that these guests interact with CB7 in slow exchange mode according to the NMR timescale. New sets of signals assigned to the 1-adamantyl cage, which appeared in the course of addition of CB7 solution, were significantly shifted to a higher field (for spectra, see Figure 3 (left) and Figures S23, S29, S35 and S41). This observation implies the inclusion of the adamantyl binding site into the CB7 cavity.<sup>24</sup> Guests **9d** and **10d**, which consist of 3,5-dimethyladamantyl cages, also form a supramolecular complex with CB7. However, in this case, only one set of guest signals was observed within the titration experiment to indicate a fast exchange binding mode. In contrast to the guest based on singly substituted adamantane cages, the Me—N and all (benz)imidazolium hydrogen signals of the guests **9d** and **10d** were shifted upfield while the signals of the H-atoms at the 1,3-dimethyladamantane cage were shifted downfield (Figure 3, right and Figures S47 and S53). Therefore, we infer that CB7, which is more rigid than  $\beta$ -CD, encapsulates predominantly (benz)imidazolyl parts of guests while 1,3-dimethyladamantyl is located close to the CB7 portals. These results are interesting from a mechanistic point of view. Masson demonstrated that ammonium cations are passed through the CB $n$  cavity in a deprotonated form.<sup>25</sup> Indeed, permanent cations, e.g. quaternary ammonium or imidazolium salts, cannot be discharged and must travel through the cavity in a charged form. Our results indicate that there is even an energy minimum arrangement with a cationic moiety of the guest situated inside the CB7 cavity. As can be expected considering the larger cavity of CB8, this macrocycle can encapsulate even bulkier 1,3-dimethyladamantane **9d** and **10d** cages. However, experiments with CB8 were accompanied with difficulties related to the poor solubility of CB8 in water. The titrations were performed using fine dispersion of CB8 in 50 mM NaCl solution to support dissolving of CB8 by cation-portal interactions. Nevertheless, the portion of

dissolved CB8 was very small and no changes in spectra were observed after the first addition, as can be seen in Figure 4 (line 2). In order to be able to observe the interactions between CB8 and guests **9b–9d** and **10b–10d** clearly, the mixtures were heated at 55 °C for 24 hours in NMR cuvettes prior to the  $^1\text{H}$  NMR spectra being recorded. Figure 4 shows the upfield shift of adamantane signals to imply their inclusion inside the CB8 cavity. Note that signal of C(2)—H appeared (Figure 4, left, line 3) as a result of well-known D/H exchange between the guest and  $\text{H}_2\text{O}$  molecules inside the CB8 cavity.<sup>26</sup> Finally, it should be mentioned that we detected no interaction of our guests with CB6 according to  $^1\text{H}$  NMR spectra (see Figures S22, S28, S34, S40, S46 and S52).

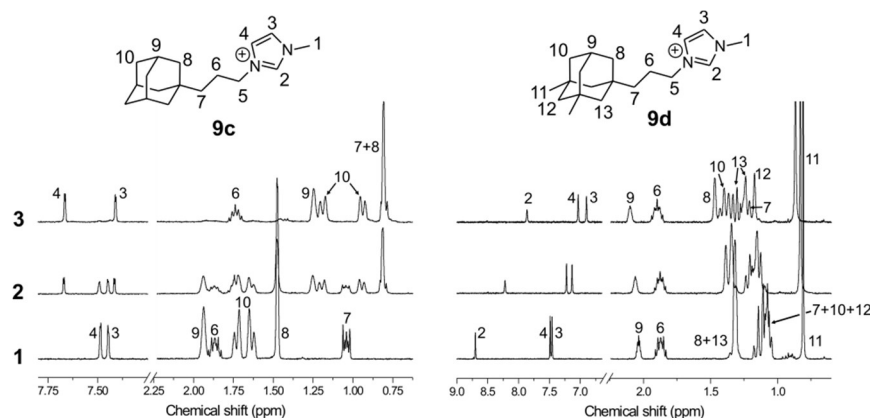


**Figure 3** Stacking plot of portions of the  $^1\text{H}$  NMR spectra recorded within titration of the guest **9c** (left) and **9d** (right) with CB7 in  $\text{D}_2\text{O}$  at 303 K. Total concentrations (in mM) of guest and CB7 were as follows: for **9c** 1.24 and 0.74 (line 1), 0.93 and 1.10 (line 2) and 0.74 and 1.33 (line 3); for **9d** 1.28 and 0.72 (line 1), 0.96 and 1.08 (line 2) and 0.77 and 1.29 (line 3), respectively.

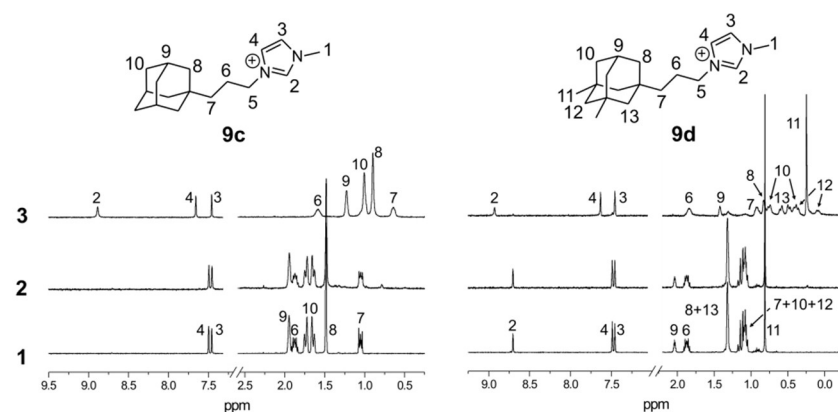


**Figure 4** Stacking plot of portions of the  $^1\text{H}$  NMR spectra recorded within titration of the guest **9c** (left) and **9d** (right) with CB8 in 50 mM NaCl solution in  $\text{D}_2\text{O}$  at 303 K. Total concentrations (in mM) of guest and CB8 were as follows: for **9c** 1.29 and 0.75 (line 1), 0.97 and 1.12 (line 2) and 0.75 and 1.33 (line 3); for **9d** 1.28 and 0.72 (line 1), 0.96 and 1.08 (line 2) and 0.77 and 1.29 (line 3), respectively.

2) and 0.77 and 1.35 (line 3); for **9d** 1.23 and 0.75 (line 1), 0.93 and 1.12 (line 2) and 0.74 and 1.35 (line 3), respectively.

### 2.2.2 Titration calorimetry

The initial intention of our work was to find new binding motifs, which can be used instead of adamantylmethyl. Therefore, we determined the association constants of new model guests (**9b–9d**, **10b–10d**) using ITC and compared the values with previously reported results for the guests **9a** and **10a**.<sup>21</sup> ITC results (Table 2) confirmed 1:1 stoichiometry of all examined complexes (see Table S1 and Figure S95–S112 for complete titration data). The  $pK$  values of all tested adamantane-based guests with  $\beta$ -CD were observed within a range of 4.7–5.7. However, the values clearly increased with prolongation of the linker between the adamantane cage and (benz)imidazolium moiety (all discussed trends can be seen in Figure 5). It is worth noting that this increase was higher in the benzimidazolia series, i.e. 10 $\times$  from **10a** to **10c** and only 7.1 $\times$  from **9a** to **9c**. This phenomenon could be attributed to the bulkier benzimidazolium core, which more negatively affects the binding strength sitting closer to the CD portal. The size of the guest also positively correlates with the  $K$  values of binding to  $\gamma$ -CD, which varied from  $8.9 \times 10^2 \text{ M}^{-1}$  for **9b** to  $8.4 \times 10^4 \text{ M}^{-1}$  for **10c**. It should be noted that bindings of all examined guests with  $\gamma$ -CD are entropy-driven with minimal enthalpy contribution. Finally, we tested the smallest member of the cyclodextrin family, i.e.  $\alpha$ -CD, to observe  $K$  values in the range of 270–500  $\text{M}^{-1}$ .

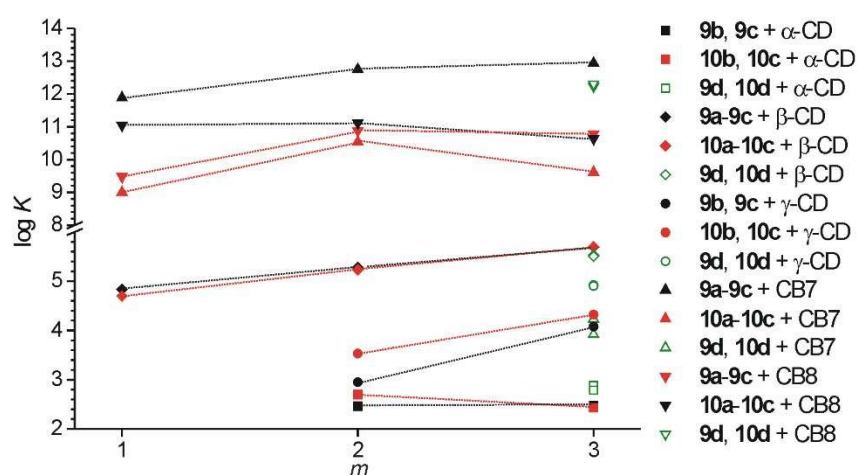


**Figure 5** Plot of  $\log K$  against the number of C-atoms ( $m$ ) in the linker between the adamantane cage and the cationic moiety of the guest (see Figure 1 for guest structures).

Considering the affinity of positively charged adamantane-based guests towards CB7, we should reflect on the contribution of host/guest desolvation and ion-dipole interactions. It is well-known that the adamantane cage perfectly fits the interior cavity of CB7. Within a complex, the centre of gravity of the adamantane cage is located close to the centre of gravity of the CB7 macrocycle and any movement of the adamantane cage along the virtual  $C_7$  axis of CB7 increases the complex energy significantly. The contribution of this hydrophobic effect has been quantified as approximately  $10^8 \text{ M}^{-1}$ .<sup>27</sup> The ion-dipole interaction can contribute approximately  $10^3 \text{ M}^{-1}$  for single cation optimally positioned in the CB7 portal. Prolongation of the linker between the adamantane cage and cationic moiety should lead to lowering of the ion-dipole contribution. Therefore, we were surprised that  $K$  value increased from  $7.6 \times 10^{11} \text{ M}^{-1}$  for **9a** to  $8.6 \times 10^{12} \text{ M}^{-1}$  for **9c**. This phenomenon can be attributed to the flexible linker, which can be bent to allow the cation reaching a position closer to the portal. An exception to this trend was observed in the benzimidazolium series where the bulky benzimidazolium cation most likely hindered the better orientation of the cation of the guest **10c** within the CB7 portal. The titration experiments with CB8 are in concert with a well-known fact that the 3,5-dimethyladamantane cage shows high selectivity towards CB7/CB8.<sup>14</sup> Thus, the guest **9d** and **10d** display the  $\log(K_{\text{CB8}}/K_{\text{CB7}})$  value of 8.3 and 8.1, respectively. It should be noted that the inclusion complexes were reported for 3,5-dimethyladamantaneamine ( $\log(K_{\text{CB8}}/K_{\text{CB7}})=7.2$ ) in a previous publication from Isaacs.<sup>14</sup> In contrast, our guests **9d** and **10d** bind the CB7 macrocycle at the (benz)imidazoliumalkyl site as NMR data suggested. However, the binding strength of our guests **9d** and **10d** towards CB7 match that of memantine,<sup>14</sup> i.e.  $\log K \sim 10^4 \text{ M}^{-1}$ , and it is approximately 10× higher towards CB8.

**Table 2** ITC results.

guest	host	$K$ [ $\text{dm}^3 \cdot \text{mol}^{-1}$ ]	$-\Delta H$ [ $\text{kJ} \cdot \text{mol}^{-1}$ ]	$\Delta S$ [ $\text{kJ} \cdot \text{mol}^{-1} \cdot \text{K}^{-1}$ ]
<b>9a</b>	$\beta$ -CD <sup>a</sup>	$(6.8 \pm 0.3) \times 10^4$	$31.4 \pm 1.8$	-11.1
	CB7 <sup>a</sup>	$(7.6 \pm 0.5) \times 10^{11 \text{ c}}$	$91.3 \pm 1.2$	-54.7
	CB8 <sup>b</sup>	$(1.1 \pm 0.1) \times 10^{11 \text{ d}}$	$53.1 \pm 1.1$	36.4
<b>9b</b>	$\alpha$ -CD	$2.9 \times 10^2$	21	22
	$\beta$ -CD	$(1.9 \pm 0.5) \times 10^5$	$31.3 \pm 0.2$	-2.4
	$\gamma$ -CD	$8.9 \times 10^2$	1.2	52.8
	CB7	$(5.6 \pm 0.8) \times 10^{12 \text{ c}}$	$89.4 \pm 1.3$	-50.9
	CB8 <sup>b</sup>	$(1.3 \pm 0.3) \times 10^{11 \text{ d}}$	$52.3 \pm 0.9$	40.2
<b>9c</b>	$\alpha$ -CD	$3.0 \times 10^2$	26	-39
	$\beta$ -CD	$(4.9 \pm 0.1) \times 10^5$	$33.21 \pm 0.15$	-0.6
	$\gamma$ -CD	$1.2 \times 10^4$	-0.9	81.2
	CB7	$(8.6 \pm 0.4) \times 10^{12 \text{ c}}$	$85.7 \pm 1.4$	-35.3
	CB8 <sup>b</sup>	$(4.3 \pm 0.9) \times 10^{10 \text{ d}}$	$49.5 \pm 1.2$	40.2
	$\alpha$ -CD	$7.7 \times 10^2$	35	-59

<b>9d</b>	$\beta$ -CD	$(3.4\pm 0.1)\times 10^5$	$39.6\pm 0.9$	-24.6
	$\gamma$ -CD	$8.4\times 10^4$	12.6	52.8
	CB7	$(8.3\pm 1.5)\times 10^3$	$18.2\pm 0.2$	14.9
	CB8 <sup>b</sup>	$(1.7\pm 0.4)\times 10^{12\ e}$	$67.3\pm 1.2$	12.0
<b>10a</b>	$\beta$ -CD <sup>a</sup>	$(5.0\pm 0.4)\times 10^4$	$27.3\pm 1.3$	0.1
	CB7 <sup>a</sup>	$(1.0\pm 0.6)\times 10^{9\ f}$	$89\pm 3$	-120.7
	CB8 <sup>b</sup>	$(3.0\pm 0.4)\times 10^{9\ d}$	$48.6\pm 1.9$	40.4
<b>10b</b>	$\alpha$ -CD	$5.0\times 10^2$	14	5
	$\beta$ -CD	$(1.7\pm 0.3)\times 10^5$	$30.2\pm 0.2$	0.5
	$\gamma$ -CD	$3.4\times 10^3$	5.3	50.2
	CB7	$(3.4\pm 0.3)\times 10^{10\ f}$	$89\pm 3$	-68.5
	CB8 <sup>b</sup>	$(7.5\pm 1.4)\times 10^{10\ d}$	$50.9\pm 1.1$	41.1
<b>10c</b>	$\alpha$ -CD	$2.7\times 10^2$	28	-46
	$\beta$ -CD	$(5.0\pm 0.1)\times 10^5$	$32.3\pm 0.4$	-33.1
	$\gamma$ -CD	$2.1\times 10^4$	-1.19	86.7
	CB7	$(4.1\pm 1.1)\times 10^{9\ f}$	$84\pm 4$	-92.4
	CB8 <sup>b</sup>	$(5.9\pm 0.8)\times 10^{10\ d}$	$50.7\pm 1.0$	37.5
<b>10d</b>	$\alpha$ -CD	$6.1\times 10^2$	36	-65
	$\beta$ -CD	$(3.2\pm 0.1)\times 10^5$	$39.8\pm 1.5$	-25.9
	$\gamma$ -CD	$8.0\times 10^4$	12.2	53.6
	CB7	$(1.7\pm 0.1)\times 10^4$	$26.9\pm 0.6$	-7.6
	CB8 <sup>b</sup>	$(2.0\pm 0.3)\times 10^{12\ e}$	$67.7\pm 1.3$	12.0

<sup>a</sup> According to the previously published paper.<sup>21</sup> Experiments were conducted in water at 303.15 K unless otherwise stated. <sup>b</sup> Performed in 50 mM NaCl solution. Competitors were used as follows: <sup>c</sup> 1,6-hexamethylenediamine·2HCl, <sup>d</sup> methyl viologen dichloride, <sup>e</sup> amantadine·HCl, <sup>f</sup> L-phenylalanine.

### 2.2.3 Mass-spectrometry

To support our hypotheses regarding complex formation and stoichiometry by an additional independent method, we analysed binary mixtures of ligands and macrocycles using ESI-MS. In all cases, we clearly observed signals related to the 1:1 complexes as can be seen in Figures S55–S78. Table S2 lists the calculated and experimental  $m/z$  values for  $[G@H]^+$ . The complexes with  $\alpha$ -CD were the only exception since we were not able to optimise experimental conditions to observe such weak supramolecular aggregates. Interestingly, we observed only one fragmentation pathway of the guest bound within the complex with CB7 instead of two pathways, which were observed for free guests. As displayed for the guest **9c** in Scheme S1, the guest molecular cation ( $m/z$  259) can release either neutral 3-(1-adamantyl)prop-1-ene to produce methylimidazolium cation ( $m/z$  83) or neutral methylimidazole to produce 1-adamantylpropyl cation ( $m/z$  177). Figure 6a shows the corresponding MS and tandem MS<sup>2</sup>. This fragmentation pattern is the same for all the guests **9b–9d** and **10b–10d**. In contrast, ion related to the **9c**@CB7 ( $m/z$  1421) release exclusively neutral 3-(1-adamantyl)prop-1-ene to produce methylimidazolium@CB7 ( $m/z$  1245) as can be seen in Figure 6b. We previously demonstrated that imidazolium salts with a molecular structure allowing slippage of the CB7

unit along the molecular axle but away from the adamantane cage strongly prefer releasing of the neutral adamantane fragment and keeping the positive charge on the imidazolium moiety.<sup>19</sup>

These results concert with the hypothesis that ion-dipole interactions play a much more critical role than the hydrophobic effect in the gas phase; though, the contribution of the hydrophobic effect is much higher than that of ion-dipole interactions in water environments.

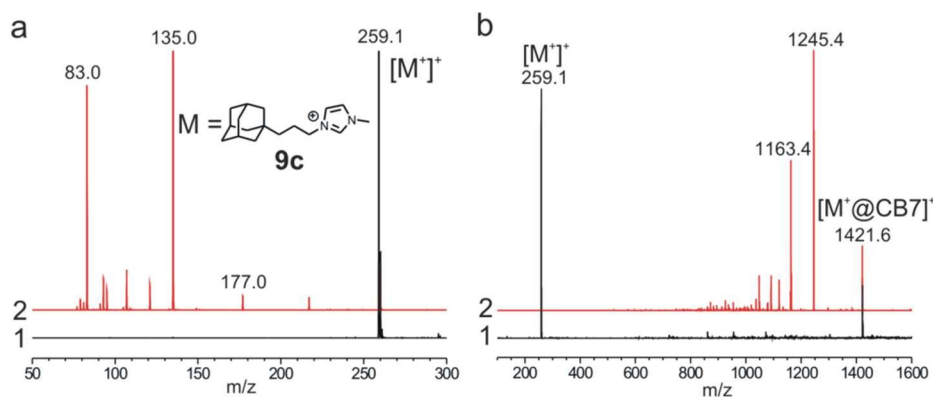


**Figure 6** Mass spectra recorded for the guest **9c** (a) and its 1:1 mixture with CB7 (b) in water. The first-order mass spectra (1), MS/MS tandem mass spectra (2).

### 3. Conclusion

This study aimed to examine whether adamantylalkyl(methyl)imidazolium binding motifs with ethylene and propylene linkers between the adamantane cage and (benz)imidazolium cation have appropriate supramolecular properties to be used instead of homologues with shorter methylene linkers for the construction of more complex multitopic guests since longer linkers are more convenient from a synthetic point of view. Therefore, we prepared a series of new adamantylated (benz)imidazolium salts and described their supramolecular properties using NMR, ITC, and mass spectrometry. Combining data from these experiments, we can conclude that all synthesised guests, i.e. **9b–9d** and **10b–10d**, form 1:1 complexes with  $\alpha$ -CD,  $\beta$ -CD,  $\gamma$ -CD, CB7 and CB8. The binding strength of cyclodextrins decreases in the order  $\beta$ -CD >  $\gamma$ -CD >  $\alpha$ -CD and the values of the association constants are in orders of magnitude of  $10^5 \text{ M}^{-1}$ ,  $10^3$ – $10^4 \text{ M}^{-1}$  and  $10^2 \text{ M}^{-1}$ , respectively.

Initially, we assumed that prolongation of the linker between the adamantane cage and cationic moiety could decrease the contribution of the ion-dipole interaction and, consequently, the stability of the complex with CB $n$ . However, our results do not display such a trend. Even, some ligands with longer linkers bind the CB $n$  stronger than a corresponding ligand with methylene linker (see, for instance, **9b**@CB7/8, **9c**@CB7, **10b**@CB7/8, **10c**@CB7/8). We infer that this

phenomenon can be related to the better accommodation of the more flexible guest to optimise ion-dipole contributions.

Finally, we conclude that new binding motifs, i.e. 1-adamantylalkyl(benz)imidazolia and 3,5-dimethyladamantan-1-ylalkyl(benz)imidazolia, are suitable candidates which can be used for the construction of more complex supramolecular components as an alternative to adamantylmethyl homologues.

## 4. Experimental Section

### 4.1 General

All solvents, reagents and starting compounds (if not mentioned otherwise) were of analytical grade, purchased from commercial sources and used without further purification. 1-(1-Adamantylalkyl)imidazole and 1-(1-adamantylalkyl)benzimidazole were prepared as described previously. Melting points were measured on a Kofler block and are uncorrected. Elemental analyses (C, H and N) were determined with a Thermo Fisher Scientific Flash EA 1112. NMR spectra were recorded at 303 K on a Bruker Avance III 500 spectrometer operating at frequencies of 500.11 MHz ( $^1\text{H}$ ) and 125.77 MHz ( $^{13}\text{C}$ ) and on a Bruker Avance III 300 spectrometer operating at frequencies of 300.13 MHz ( $^1\text{H}$ ) and 75.77 MHz ( $^{13}\text{C}$ ).  $^1\text{H}$  and  $^{13}\text{C}$  NMR chemical shifts were referenced to the signal of the solvent [ $^1\text{H}$ :  $\delta(\text{residual HDO}) = 4.70$  ppm,  $\delta(\text{residual DMSO-}d_5) = 2.50$  ppm;  $^{13}\text{C}$ :  $\delta(\text{DMSO-}d_6) = 39.52$  ppm]. The spin-lock for ROESY was adjusted to 400 ms. The signal multiplicity is indicated by “s” for singlet, “d” for doublet, “t” for triplet, and “um” for unresolved multiplet. IR spectra were recorded using a Smart OMNI-Transmission Nicolet iS10 spectrophotometer. Samples were measured in KBr pellets. Electrospray mass spectra (ESI-MS) were recorded using an amaZon X ion-trap mass spectrometer (Bruker Daltonics, Bremen, Germany) equipped with an electrospray ionisation source. All the experiments were conducted in the positive-ion polarity mode. The instrumental conditions used to measure the single (benz)imidazolium salts and their mixtures with the host molecules were different; therefore, they are described separately. *Single (benz)imidazolium salts*: Individual samples (with concentrations of  $0.5 \mu\text{g}\cdot\text{cm}^{-3}$ ) were infused into the ESI source in methanol:water (1:1, v:v) solutions using a syringe pump with a constant flow rate of  $3 \mu\text{l}\cdot\text{min}^{-1}$ . The other instrumental conditions were as follows: an electrospray voltage of  $-4.2$  kV, a capillary exit voltage of 140 V, a drying gas temperature of  $220^\circ\text{C}$ , a drying gas flow rate of  $6.0 \text{ dm}^3\cdot\text{min}^{-1}$  and a nebulizer pressure of 55.16 kPa. *Host-guest complexes*: An aqueous solution of the guest molecule ( $6.25 \mu\text{M}$ ) and the corresponding host molecule (1.0 eq of CBn and 3.0 eq of CD, respectively) was infused into the ESI source at a constant flow rate of  $3 \mu\text{l}\cdot\text{min}^{-1}$ . The other instrumental conditions were as follows: an electrospray voltage of  $-4.0$  kV, a capillary exit voltage of 140 V up to  $-50$  V, a drying gas temperature of  $300^\circ\text{C}$ , a drying gas flow rate of  $6.0 \text{ dm}^3\cdot\text{min}^{-1}$ , and a nebuliser pressure of 206.84 kPa. Nitrogen was used as both the nebulising and drying gas for all of the experiments. Tandem mass spectra were collected using CID with He as the collision gas after the isolation of the required ions. Isothermal titration calorimetry measurements were carried out in  $\text{H}_2\text{O}$  using a VP-ITC MicroCal instrument at 303 K. The concentrations of the host in the cell and the guest in the microsyringe were approximately 0.13–0.15 and 0.46–0.50 mM, respectively. The raw experimental data were analysed with the MicroCal ORIGIN software. The heats of dilution were taken into account for each guest compound. The data were fitted to a theoretical titration curve using the ‘One Set of Binding Sites’ model. A 1,6-hexamethylenediamine $\cdot$ 2HCl (HMDCI), L-phenylalanine, methyl viologen dichloride ( $\text{MV}\cdot 2 \text{ HCl}$ ), and amantadine $\cdot$ HCl

with respective association constants  $K_{CB7}=2.05\times 10^9\text{ M}^{-1}$ ,  $K_{CB7}=5.16\times 10^5\text{ M}^{-1}$ ,  $K_{CB8}=7.05\times 10^6\text{ M}^{-1}$ ,  $K_{CB8}=2.89\times 10^9\text{ M}^{-1}$  were used as competitors. The complexation enthalpies for the multistep titration experiments were calculated as the sum of the enthalpies of each complexation step. The values of  $K$  obtained from the competitive titrations were verified using different concentrations of competitors. All titrations with CB7, CB8 and  $\beta$ -CD were performed in triplicate. Titrations with  $\alpha$ -CD and  $\gamma$ -CD were performed only once.

### 3-(3,5-dimethyladamantan-1-yl)-1-propanol (**6c**)

3-(3,5-Dimethyladamantan-1-yl)propionic acid (1.504 g, 6.36 mmol) was prepared from 1-bromoadamantane according to the literature.<sup>22,23</sup> Subsequently, alcohol **6c** was prepared according to a protocol reported by Babjaková *et al.*<sup>20</sup> to get a colourless oil (1.267 g, 90 %).  $^1\text{H NMR}$  (400 MHz,  $\text{CDCl}_3$ ):  $\delta$  0.81 (m, 6H), 1.05–1.15 (um, 8H), 1.31 (m, 6H), 1.53 (m, 2H), 2.0 (m, 1H), 3.61 (t, 2H,  $J=13.6$  Hz) ppm.  $^{13}\text{C}\{^1\text{H}\}$  NMR ( $\text{CDCl}_3$ ):  $\delta$  26.1, 29.8, 30.7, 31.2, 33.7, 39.7, 41.0, 43.4, 48.9, 51.3, 64.0 ppm. IR: 457 (w), 507 (w), 533 (w), 668 (w), 698(m), 753 (w), 889 (w), 920 (w), 938 (w), 962 (m), 1011 (m), 1059 (s), 1154 (w), 1170 (w), 1256 (w), 1341 (m), 1357 (m), 1373 (m), 1454 (s), 1635 (w), 2839–2942 (bs), 3364 (bs)  $\text{cm}^{-1}$ . MS (EI: 200°C, 70eV): 41(9), 55(9), 91(11), 93(12), 95(5), 105(10), 107(53), 108(5), 121(7), 163(100), 164(13) m/z (%).

### 3-(3,5-dimethyladamantan-1-yl)-1-bromopropane (**7c**)

Alcohol **6c** (0.2000 g, 0.90 mmol) was dissolved in dry  $\text{CH}_2\text{Cl}_2$  (30  $\text{cm}^3$ ) under inert atmosphere and cooled down to 0 °C in an ice bath.  $\text{CBr}_4$  (1.0090 g, 3.04 mmol) was added followed by the addition of triphenylphosphine (1.260 g, 4.81 mmol) in small portions. The mixture was stirred for 3 h at 0 °C and then poured into cold pentane and stirred for 20 min. The liquid phase was evaporated to dryness and the solid was washed with cold pentane. Pentane fractions were evaporated and purified by column chromatography on silica gel using petroleum ether as a mobile phase to get colourless oil **7c** (0.2010 g, 78%).  $^1\text{H NMR}$  (400 MHz,  $\text{CDCl}_3$ ):  $\delta$  0.81 (m, 6H), 1.01–1.14 (um, 6H), 1.12 (m, 2H), 1.30 (m, 6H), 1.83 (m, 2H), 2.05 (m, 1H), 3.37 (t, 2H,  $J=14.0$  Hz) ppm.  $^{13}\text{C}\{^1\text{H}\}$  NMR ( $\text{CDCl}_3$ ):  $\delta$  26.7, 29.8, 30.6, 31.2, 33.8, 34.9, 41.0, 42.4, 43.4, 48.8, 51.3 ppm. IR: 409 (w), 465 (w), 561 (m), 645 (w), 657 (m), 721(w), 736 (w), 754 (w), 778 (w), 810 (m), 836 (w), 913 (m), 938 (w), 970 (w), 990 (w), 1037 (w), 1098 (m), 1179 (w), 1207 (m), 1241 (m), 1256 (m), 1272 (m), 1287 (w), 1298 (w), 1316 (w), 1346 (w), 1361 (w), 1346 (w), 1361 (w), 14451 (bm), 2635 (w), 2656 (w), 2672 (w), 2751 (w), 2900 (bs)  $\text{cm}^{-1}$ . MS (EI: 200°C, 70eV) 41(13), 55(9), 79(7), 81(5), 91(11), 93(10), 105(8), 107(45), 163(100), 164(13), 269(1), 271(1) m/z (%).

### 1-(2-(1-adamantyl)ethyl)benzimidazole (**9**)

The benzimidazole (146 mg, 1.24 mmol) was dissolved in dry DMF (7.5  $\text{cm}^3$ ) and sodium hydride (60 % dispersion in mineral oil, 79 mg, 1.98 mmol) was added. When gas evolution stopped, 2-(1-adamantyl)-1-bromoethane (**7a**) (200 mg, 8.22 mmol) was added. The mixture was heated at 80 °C for 24 h. The reaction mixture was poured on ice and extracted  $3\times 5\text{ cm}^3$  with dichloromethane. The combined extract was washed with water, dried over  $\text{Na}_2\text{SO}_4$  and evaporated. The title compound was obtained as a colourless solid (180 mg, 78%). M.p.: 128–133 °C. Calcd. for  $\text{C}_{19}\text{H}_{24}\text{N}_2$  (280.41) C 81.38, H 8.63, N 9.99 (%). Found C 81.15, H 8.72, N 9.85 (%).  $^1\text{H NMR}$  (500 MHz,  $\text{CDCl}_3$ ):  $\delta$  1.62 (m, 6H), 1.66 (m, 5H), 1.77 (m, 3H), 2.03 (m, 3H), 4.18 (m, 2H), 7.31 (m, 2H), 7.39 (d, 1H,  $J=7.5$  Hz), 7.81 (d, 1H,  $J=8.0$  Hz), 7.94 (s, 1H) ppm.  $^{13}\text{C}\{^1\text{H}\}$  NMR ( $\text{CDCl}_3$ ):  $\delta$  28.4, 29.6, 32.0, 36.9, 40.1, 42.2, 43.9, 109.6, 120.3, 122.0, 122.7, 133.6, 142.6, 143.6 ppm. IR: 430 (w), 480 (w), 469 (w), 631 (w), 640 (w), 669 (w), 740 (s), 768 (w), 779 (w), 813 (w), 878 (w), 889 (w), 926 (w), 973 (w), 1005 (w), 1057 (w), 1097 (w), 1161 (m), 1200(m), 1240 (m), 1273 (w), 1288 (m), 1331 (w), 1346 (w), 1365 (w), 1365

(m), 1385 (s), 1452 (s), 1496 (s), 1585 (w), 1616 (w), 1747 (w), 1770 (w), 1884 (w), 1921 (w), 2345 (w), 2846 (s), 2902 (s), 2918 (s), 2979 (w), 3033 (w), 3050 (w), 3095 (w)  $\text{cm}^{-1}$ . ESI-MS:  $m/z$  281.3  $[\text{M}]^+$ .

*1-(2-(1-adamantyl)ethyl)-3-methylbenzimidazolium iodide (10b)*

1-(2-(1-adamantyl)ethyl)benzimidazole (**9**) (200 mg, 71 mmol) was dissolved in methyl iodide (4.56 g, 32.13 mmol). The mixture was heated at 80 °C and after 24 h it was cooled to room temperature. The product was precipitated by the addition of diethyl ether, washed by THF and dried using reduced pressure. Compound **10b** was obtained as a colourless solid 200 mg (66%). M.p.: 153–158 °C. Calcd. for  $\text{C}_{20}\text{H}_{27}\text{N}_2\text{I}\cdot 1.5 \text{H}_2\text{O}$  (449.37) C 53.46, H 6.73, N 6.23 (%). Found C 53.48, H 6.38, N 6.22 (%).  $^1\text{H}$  NMR (400 MHz,  $\text{DMSO}-d_6$ ):  $\delta$  1.62 (m, 6H), 1.72 (um, 8H), 1.98 (m, 3H), 4.07 (s, 3H), 4.49 (m, 2H), 7.71 (m, 2H), 8.03 (m, 2H), 9.76 (s, 1H) ppm.  $^{13}\text{C}\{^1\text{H}\}$  NMR ( $\text{DMSO}-d_6$ ):  $\delta$  27.8, 31.7, 33.2, 36.4, 41.4, 42.1, 42.4, 113.4, 113.5, 126.4, 130.8, 131.8, 142.5 ppm. IR: 424 (w), 559 (w), 602 (w), 669 (w), 762 (s), 849 (w), 1012 (w), 1063 (w), 1097 (w), 1130 (w), 1163 (w), 1203 (w), 1221 (w), 1255 (m), 1281 (w), 1346 (m), 1385 (w), 1448 (m), 1461 (m), 1489 (w), 1567 (s), 1618 (w), 1655 (w), 1805 (w), 1846 (w), 2345 (w), 2362 (w), 2645 (w), 2674 (w), 2846 (s), 2898 (s), 3014 (m), 3043 (m), 3137 (w), 3442 (bs), 3502 (bs)  $\text{cm}^{-1}$ . ESI-MS:  $m/z$  295.3  $[\text{M}]^+$ .

*1-(2-(1-adamantyl)ethyl)-3-methylimidazolium bromide (9b)*

Compound **7a** (200 mg, 0.82 mmol) and 1-methylimidazole (81 mg, 0.99 mmol) were heated under inert atmosphere in dry acetonitrile (5  $\text{cm}^3$ ) at 82 °C for 168 h. The reaction mixture was cooled down and freshly distilled diethyl ether was added at room temperature. The precipitate was centrifuged, washed with diethyl ether (3 $\times$ 10  $\text{cm}^3$ ) and dried in vacuo to get 148 mg (55%) of **9b** as a colourless solid. M.p.: 188–189 °C. Calcd. for  $\text{C}_{16}\text{H}_{25}\text{BrN}_2\cdot 2.1 \text{H}_2\text{O}$  (363.12) C 52.92, H 8.11, N 7.71 (%). Found C 52.85, H 7.87, N 7.74 (%).  $^1\text{H}$  NMR (400 MHz,  $\text{DMSO}-d_6$ ):  $\delta$  1.52 (m, 6H), 1.66 (um, 8H), 1.94 (m, 3H), 3.85 (s, 3H), 4.19 (m, 2H), 7.71 (s, 1H), 7.82 (s, 1H), 9.25 (s, 1H) ppm.  $^{13}\text{C}\{^1\text{H}\}$  NMR ( $\text{DMSO}-d_6$ ):  $\delta$  27.8, 31.6, 35.7, 36.3, 39.3, 41.4, 43.5, 44.4, 122.3, 123.4, 136.5 ppm. IR: 619 (m), 666 (w), 767 (w), 813 (w), 965 (w), 972 (w), 1020 (w), 1104 (w), 1169 (m), 1307 (w), 1318 (w), 1344 (w), 1364 (w), 1371 (w), 1428 (w), 1449 (m), 1573 (m), 1620 (w), 1630 (w), 2349 (w), 2657 (w), 2674 (w), 2846 (s), 2899 (s), 3069 (m), 3143 (m), 3450 (bs)  $\text{cm}^{-1}$ . ESI-MS:  $m/z$  245.0  $[\text{M}]^+$ ,  $m/z$  569.3  $[2\cdot\text{M}^+ + ^{79}\text{Br}^-]^+$ .

*1-(3-(1-adamantyl)propyl)-3-methylimidazolium bromide(9c)*

Compound **9c** was prepared according the same procedure as described above for **9b** using **7b** (0.344 g, 1.34 mmol) to get 0.138 g (30 %) of **9c** as a colourless solid. M.p.: 143–146 °C. Calcd. for  $\text{C}_{17}\text{H}_{27}\text{BrN}_2\cdot 0.9 \text{H}_2\text{O}$  (355.52) C 57.43, H 8.17, N 7.87 (%). Found C 57.51, H 8.02, N 7.88 (%).  $^1\text{H}$  NMR (400 MHz,  $\text{DMSO}-d_6$ ):  $\delta$  1.00 (m, 2H), 1.43 (m, 6H), 1.62 (m, 6H), 1.75 (m, 2H), 1.91 (m, 1H), 3.85 (s, 3H), 4.11 (t, 2H,  $J=7.2$  Hz), 7.69 (d, 1H,  $J=1.6$  Hz), 7.77 (d, 1H,  $J=1.6$  Hz), 9.12 (s, 1H), ppm.  $^{13}\text{C}\{^1\text{H}\}$  NMR ( $\text{DMSO}-d_6$ ):  $\delta$  23.0, 27.9, 31.5, 35.7, 36.52, 39.7, 41.7, 49.5, 122.2, 123.6, 136.5 ppm. IR: 595 (m), 605 (m), 620 (w), 649 (w), 754 (m), 810 (w), 816 (w), 840 (w), 971 (w), 1001 (w), 1008 (w), 1071 (w), 1100 (w), 1168 (s), 1227 (w), 1256 (w), 1290 (w), 1318 (w), 1343 (w), 1364 (w), 1383 (w), 1436 (m), 1565 (m), 1616 (m), 1622 (w), 2656 (w), 2670 (w), 2845 (s), 2898 (s), 2924 (s), 3074 (m), 3142 (m), 3426 (bm), 3487 (bm)  $\text{cm}^{-1}$ . ESI-MS:  $m/z$  259.1  $[\text{M}]^+$ ,  $m/z$  597.3  $[2\cdot\text{M}^+ + ^{79}\text{Br}^-]^+$ .

*1-(3-(1-adamantyl)propyl)-3-methylbenzimidazolium bromide (10c)*

Compound **10c** was prepared according the same procedure as described above for **9b** using **7b** (0.2600 g, 1.01 mmol) to get 0.3580 g (91 %) of **10c** as an off-white solid. M.p.: 122–123 °C. Calcd. for  $\text{C}_{21}\text{H}_{29}\text{BrN}_2\cdot 1.3 \text{H}_2\text{O}$  (412.79) C 61.10, H 7.72, N 6.79 (%). Found C 61.02, H 7.59,

N 6.72 (%).  $^1\text{H}$  NMR (400 MHz, DMSO- $d_6$ ):  $\delta$  1.12 (m, 2H), 1.43 (m, 6H), 1.61 (m, 6H), 1.89 (um, 5H), 4.08 (s, 3H), 4.44 (t, 2H,  $J=7.2$  Hz), 7.70 (um, 2H), 8.02 (m, 1H), 8.07 (m, 1H), 9.72 (s, 1H) ppm.  $^{13}\text{C}\{^1\text{H}\}$  NMR (DMSO- $d_6$ ):  $\delta$  22.1, 27.9, 31.6, 36.5, 39.9, 41.7, 47.2, 113.5, 113.5, 124.4, 126.5, 130.9, 131.8, 142.6 ppm. IR: 420 (w), 460 (w), 467 (m), 605 (w), 759 (s), 812 (w), 879 (w), 977(w), 1013 (w), 1026 (w), 1059 (w), 1069 (w), 1097 (w), 1102 (w), 1134 (w), 1212 (w), 1224 (w), 1268 (w), 1281 (w), 1313 (w), 1347 (m), 1355 (m), 1381 (w), 1421 (m), 1432 (s), 1450 (m), 1485 (s), 1568 (w), 1619 (m), 1991 (w), 2048 (w), 2345 (w), 2426 (w), 2446 (w), 2636 (w), 2657 (w), 2673 (w), 2843 (s), 2900 (bs), 2989 (m), 3024 (m), 3069 (w), 3137 (w), 3398 (bs), 3466 (bs)  $\text{cm}^{-1}$ . ESI-MS:  $m/z$  309.2  $[\text{M}]^+$ ,  $m/z$  697.4  $[2\cdot\text{M}^+ + ^{79}\text{Br}^-]^+$ .

#### *1-(3-(3,5-dimethyladamantan-1-yl)propyl)-3-methylimidazolium bromide (9d)*

Compound **9d** was prepared according the same procedure as described above for **9b** using **7c** (0.497 g, 1.74 mmol) to get 0.372 g (58 %) of **9d** as a colourless solid. M.p.: 179–181 °C. Calcd. for  $\text{C}_{19}\text{H}_{31}\text{BrN}_2\cdot 0.6 \text{H}_2\text{O}$  (378.18) C 60.34, H 8.58, N 7.40 (%). Found C 60.31, H 8.46, N 7.53 (%).  $^1\text{H}$  NMR (400 MHz, DMSO- $d_6$ ):  $\delta$  0.78 (s, 6H), 1.01–1.07 (um, 8H), 1.26 (um, 6H), 1.74 (m, 2H), 2.0 (m, 1H), 3.85 (s, 3H), 4.11 (t, 2H,  $J=7.2$  Hz), 7.70 (d, 1H,  $J=1.6$  Hz), 7.78 (d, 1H,  $J=1.6$  Hz), 9.12 (s, 1H), ppm.  $^{13}\text{C}\{^1\text{H}\}$  NMR (DMSO- $d_6$ ):  $\delta$  22.7, 28.9, 30.1, 30.9, 33.0, 36.1, 37.0, 40.0, 42.6, 47.9, 49.2, 50.8, 121.6, 123.7, 136.4 ppm. IR: 620 (m), 632 (m), 655 (w), 740 (w), 770 (m), 844 (bw), 1040 (w), 1163 (s), 1174 (s), 1242 (w), 1269 (w), 1303 (w), 1337 (w), 1359 (w), 1374 (w), 1381 (m), 1455 (s), 1475 (m), 1565 (s), 1636 (bw), 1747 (w), 2842 (s), 2859 (m), 2902 (s), 2938 (m), 3060 (m), 3114 (w), 3123 (w), 3151 (w), 3448 (bm)  $\text{cm}^{-1}$ . ESI-MS:  $m/z$  287.2  $[\text{M}]^+$ ,  $m/z$  653.4  $[2\cdot\text{M}^+ + ^{79}\text{Br}^-]^+$ .

#### *1-(3-(3,5-dimethyladamantan-1-yl)propyl)-3-methylbenzimidazolium bromide (10d)*

Compound **10d** was prepared according the same procedure as described above for **9b** using **7c** (0.425 g, 1.49 mmol) to get 0.356 g (57 %) of **10d** as an off-white solid. M.p.: 108–110 °C. Calcd. for  $\text{C}_{23}\text{H}_{33}\text{BrN}_2\cdot 1.5 \text{H}_2\text{O}$  (444.45) C 62.12, H 8.16, N 6.30 (%). Found C 62.13, H 7.87, N 6.31 (%).  $^1\text{H}$  NMR (400 MHz, DMSO- $d_6$ ):  $\delta$  0.77 (s, 6H), 1.04–1.09 (um, 8H), 1.26 (m, 6H), 1.87 (m, 2H), 1.99 (m, 3H), 4.08 (s, 3H), 4.43 (t, 2H,  $J=7.2$  Hz), 7.70 (um, 2H), 8.02 (m, 1H), 8.07 (m, 1H), 9.72 (s, 1H) ppm.  $^{13}\text{C}\{^1\text{H}\}$  NMR (DMSO- $d_6$ ):  $\delta$  22.4, 29.0, 30.4, 30.8, 32.9, 33.4, 39.4, 40.3, 42.8, 47.2, 48.1, 50.7, 113.4, 113.5, 126.4, 130.9, 131.8, 142.6 ppm. IR: 423 (w), 467 (w), 568 (w), 610 (w), 755 (s), 760 (m), 774 (w), 789 (w), 887 (w), 939 (w), 965 (w), 1013 (w), 1030 (w), 1101 (w), 1133 (w), 1140 (w), 1165 (w), 1215 (w), 1280 (w), 1357 (m), 1371 (m), 1421 (m), 1432 (s), 1450 (m), 1487 (w), 1570 (s), 1617 (m), 1799 (w), 2837 (s), 2861 (s), 2896 (s), 2943 (s), 3013 (m), 3072 (w), 3140 (w), 3385 (bs), 3442 (bs), 3481 (bs)  $\text{cm}^{-1}$ . ESI-MS:  $m/z$  337.2  $[\text{M}]^+$ ,  $m/z$  753.4  $[2\cdot\text{M}^+ + ^{79}\text{Br}^-]^+$ .

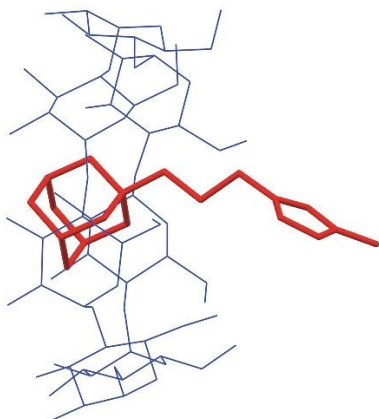
### Acknowledgements

This work was supported by the Internal Funding Agency of the Tomas Bata University in Zlín under Grant IGA/FT/2019/007.

### References

- Takata, T.; Kihara, N.; Furusho, Y. *Adv. Polym. Sci.* **2004**, *171*, 1–75.
- Yan, Z.; Huang, Q.; Liang, W.; Yu, X.; Zhou, D.; Wu, W.; Chruma, J. J.; Yeng, C. *Org. Lett.* **2017**, *19*, 898–901.
- Qu, D.-H.; Wang, Q.-C.; Tian, H. *Agnew. Chem. Int. Ed.* **2005**, *44*, 5296–5299.
- Szejtli, S. *Pure Appl. Chem.* **2004**, *76*, 1825–1845.

- <sup>5</sup> a) Marinescu, L.; Mølbach, M.; Rousseau, C.; Bols, M. *J. Am. Chem. Soc.* **2005**, *127*, 17578–17579; b) Zhu, Q., Shen, H., Yang, Z., Ji, H. *Chin. J. Cat.* **2016**, *37*, 1227–1234; c) Tabushi, I. *Acc. Chem. Res.* **1982**, *15*, 66–72; d) Bjerre, J., Fenger, H. T., Marinescu, L. G., Bols, M. *Eur. J. Org. Chem.* **2007**, 704–710; e) Shen, H.-M., Ji, H.-B. *Tetrahedron Lett.* **2012**, *53*, 3541–3545; e) Wei, X., Wu, W., Matsushita R., Yan, Z., Zhou, D., Chruma, J. J., Nishijima, M., Fukuhara, G., Mori, T., Inoue, Y., Yang, C. *J. Am. Chem. Soc.* **2018**, *140*, 3959–3974.
- <sup>6</sup> a) Armstrong, D. W.; Alak, A.; Bui, K.; Demond, W.; Ward, T.; Riehl, T. E.; Hinze, W. L. *J. Incl. Phenom.* **1984**, *2*, 533–545; b) Juvancz, Z.; Szejtli, S. *Trac-Trends Anal. Chem.* **2002**, *21*, 379–388.
- <sup>7</sup> Behrend, R.; Meyer, E.; Rusche, F. *Justus Liebig's Ann. Chem.* **1905**, *339*, 1–37.
- <sup>8</sup> Freeman, W. A.; Mock, W. L.; Shih, N.-Y. *J. Am. Chem. Soc.* **1981**, *103*, 7367–7368.
- <sup>9</sup> Kim, J.; Jung, I.-S.; Kim, S.-Y.; Lee, E.; Kang, J.-K.; Sakamoto, S.; Yamaguchi, K.; Kim, K. *J. Am. Chem. Soc.* **2000**, *122*, 540–541.
- <sup>10</sup> Mock, W. L.; Shih, N.-Y. *J. Am. Chem. Soc.* **1989**, *111*, 2697–2699.
- <sup>11</sup> Nau, W. M.; Florea, M.; Assaf, K. I. *Isr. J. Chem.* **2011**, *51*, 559–577.
- <sup>12</sup> Rekharsky, M. V.; Mori, T.; Yang, Ch.; Ko, Y. H.; Selvapalam, N.; Kim, H.; Sobransingh, D.; Kaifer, A. E.; Liu, S.; Isaacs, L.; Chen, W.; Moghaddam, S.; Gilson, M. K.; Kim, K.; Yoshihisa, I. *PNAS* **2007**, *104*, 20737–20742.
- <sup>13</sup> Moghaddam, S.; Yang, C.; Rekharsky, M.; Ko, Y. H.; Kim, K.; Inoue, Y.; Gilson, M. K. *J. Am. Chem. Soc.* **2011**, *133*, 3570–3581.
- <sup>14</sup> Liu, S. M.; Ruspici, C.; Mukhopadhyay, P.; Chakrabarti, S.; Zavalij, P. Y.; Isaacs, L. *J. Am. Chem. Soc.* **2005**, *127*, 15959–15967.
- <sup>15</sup> Cao, L. P.; Šekutor, M.; Zavalij, P. Y.; Mlinarić-Majerski, K.; Glaser, R.; Isaacs, L. *Angew. Chem., Int. Ed.* **2014**, *53*, 988–993.
- <sup>16</sup> Šekutor, M.; Molčanov, K.; Cao, L. P.; Isaacs, L.; Glaser, R.; Mlinarić-Majerski, K. *Eur. J. Org. Chem.* **2014**, 2533–2542.
- <sup>17</sup> Jelínková, K.; Surmová, H.; Matelová, A.; Rouchal, M.; Prucková, Z.; Dastychová, L.; Nečas, M.; Vícha, R. *Org. Lett.* **2017**, *19*, 2698–2701.
- <sup>18</sup> Branná, P.; Rouchal, M.; Prucková, Z.; Dastychová, L.; Lenobel, R.; Pospíšil, T.; Maláč, K.; Vícha, R. *Chem. Eur. J.* **2015**, *21*, 11712–11718.
- <sup>19</sup> Černochová, J.; Branná, P.; Rouchal, M.; Kulhánek, P.; Kuřitka, I.; Vícha, R. *Chem. Eur. J.* **2012**, *18*, 13633–13637.
- <sup>20</sup> Babjaková, E.; Branná, P.; Kuczyńska, M.; Rouchal, M.; Prucková, Z.; Dastychová, L.; Vícha, J.; Vícha, R. *RSC Advances* **2016**, *6*, 105146–105153.
- <sup>21</sup> Branná, P.; Černochová, J.; Rouchal, M.; Kulhánek, P.; Babinský, M.; Marek, R.; Nečas, M.; Kuřitka, I.; Vícha, R. *J. Org. Chem.* **2016**, *81*, 9595–9604.
- <sup>22</sup> Ohno, M.; Ishizaki, K.; Eguchi, S. *J. Org. Chem.* **1988**, *53*, 1285–1288.
- <sup>23</sup> Tanaka, K.; Hiraoka, T.; Ishiguro, F.; Jeon, J.-H.; Chujo, Y. *RSC Adv.*, **2014**, *4*, 28107–28110.
- <sup>24</sup> a) Barrow, S. J.; Kaseira, S.; Rowland, M. J.; Barrio, J.; Scherman, O. A. *Chem. Rev.* **2015**, *115*, 12320–12406; b) Assaf, K. I.; Nau, W. M. *Chem. Soc. Rev.* **2015**, *44*, 394–418.
- <sup>25</sup> Ling, X.; Samuel, E. L.; Patchel, D. L.; Masson, E. *Org. Lett.* **2010**, *12*, 2730–2733.
- <sup>26</sup> a) Wang, R.; Yuan, L.; Macartney, D. H. *Chem. Commun.* **2006**, 2908–2910; b) Li, S.; Wyman, I. W.; Wang, C.; Wang, Y.; Macartney, D. H.; Wang, R. *J. Org. Chem.* **2016**, *81*, 9494–9498.
- <sup>27</sup> Nau, W. M.; Florea, M.; Assaf, K. I. *Isr. J. Chem.* **2011**, *51*, 559–577.

**For Table of Contents**

**Adamantane-based imidazolium salts** with flexible linkers between the adamantane cage and imidazolium moiety were synthesised. Supramolecular behaviour towards natural cyclodextrins  $\alpha$ -CD,  $\beta$ -CD and  $\gamma$ -CD and cucurbit[*n*]urils ( $n=7,8$ ) was studied.